Case Studies in Thermal Engineering 8 (2016) 300–310

Contents lists available at ScienceDirect

Case Studies in Thermal Engineering

journal homepage: www.elsevier.com/locate/csite

Optimal control of batch cooling crystallizers by using genetic algorithm

Younes Amini [a,*], M. Barzegar Gerdroodbary [b], Mahmoud Reza Pishvaie [c], Rasoul Moradi [d], S. Mahruz Monfared [c]

[a] Department of Chemical Engineering, Isfahan University of Technology, Isfahan, Iran
[b] Department of Mechanical Engineering, Babol University of Technology, Babol, Iran
[c] Department of Chemical and Petroleum Engineering, Sharif University of Technology, Tehran, Iran
[d] Transport Phenomena & Nanotechnology Lab., School of Chemical Engineering, College of Engineering, University of Tehran, Tehran, Iran

ARTICLE INFO

Article history:
Received 15 May 2016
Received in revised form
11 August 2016
Accepted 2 September 2016
Available online 3 September 2016

Keywords:
Batch cooling crystallization
Population balance
Genetic algorithm
Optimal control

ABSTRACT

The formation of crystals from solutions plays a key role in various industrial applications. In this study, a new approach is presented into the optimal control of batch cooling crystallizers through a genetic algorithm. The Population balance is formularized for a typical batch crystallizer. The objective functions considered here are related to quality of products at the end of the batch. These functions are objective function of maximum mean weight size, closeness to the specified value and minimum coefficient of variation. By using an optimization algorithm (genetic algorithm), the minimum and maximum values of the objective function the input temperature parameter are obtained. The obtained results show that various trajectories can be used for cooling batch crystallizer based on objective functions. This method is applied for the potassium-nitrate system.

1. Introduction

Crystallization of organic and inorganic substances in solutions is one of the essential processes in different industrial applications including chemical, electronics and pharmaceutical industries [1–3]. This process provides highly purified products that are highly demanded by a noticeable fraction of industrial markets. In addition, crystallization presents a practical method for obtaining pure chemical substances in a satisfactory condition for packing and storing [4,5]. In the chemical engineering process, this method gains great advances except in some aspects such as the overall control on the temperature of crystallites to obtain the appropriate shape and size of particles [6,7]. Although high purity of products seems an important objective in the crystallization, the appearance and size of a crystalline product is also significant parameters. The reasonable size and size uniformity are desirable for filtering, washing, reacting, transporting and storing of the crystals [8]. As the crystals are processed further in optimized temperature, the size of the particles becomes uniform in the whole solution [9]. If the crystals are a final product of marketing, crystals with strong, non-aggregated, uniform in size, and non-caking is highly important in the packing. For these reasons, crystal size distribution (CSD) must form under a precise temperature control. In fact, the appropriate temperature control plays a significant role in the design and operation of crystallizers [10].

* Corresponding author.
E-mail address: y.amini@ce.iut.ac.ir (Y. Amini).

http://dx.doi.org/10.1016/j.csite.2016.09.001

Nomenclature

A	hear transfer surface
B	nucleation rate, number/g-solvent min
b	nucleation power
C	concentration of solute, g/g-solution
C_{0i}	nitial concentration
C_{sat}	saturated solution, g/g-solution
C_p	heat capacity of solution J/(kg. K)
f	population density function
G	growth rate, m/min
g	growth power
$\hat{H}_*$	partial molar enthalpy
$\hat{H}$	specific enthalpy
H_{ext}	exited heat flux
K_E	kinetic energy
k_b	nucleation coefficient
k_g	growth coefficient
k_v	volumetric shape factor
L	crystal size (m)
L_{wm}	mean weight size
m	crystal mass
n	number of moles
P	pressure
P_E	potential energy, J
Q	volume floe rate
S	super saturation
t	time
T	temperature
U	heat transfer coefficient
V	volume of crystallizer, m^3
w	Gaussian function weight

Greek symbols

ρ	density (g/ cm3)
δ	*Dirac function*
μ_j	j-th moment of the CSD
σ	standard deviation
σ^2	variance

Subscripts

k	index of flow
c	crystal

To obtain these goals, the batch reactors (crystallizers) have to be operated optimally in a precise condition. Hence, the main problem on the control of batch crystallizer is the optimization strategies. To overcome in this problem, some researchers have expressed the procedures to find a temperature that optimizes the final distribution of particle sizes [11–15]. In fact, due to the experimental limitations, simulation and theoretical optimization possess the greatest value to achieve the optimal control of the batch reactor. Simulation and theoretical optimization, as a research tool, can complete the results of experimental studies by calculating the desired parameters at regions or situations in which experimental work is expensive or impossible [16–27]. In the past few decades, iterative model development, and experimental designs have been employed in some crystallization processes. Gunawan et al. [28] have reported a model for different growth rates of crystallites in the batch reactor. In the other investigations, Ma and Braatz [29,30] have used the overall closed loop crystal product as the objective of the experimental design. Furthermore, various efforts have been performed on the optimal control of the batch cooling crystallizers that are reported in various literatures [31–33]. The influence of the crystal size distribution and degree of freedom on the performance of crystallization was studied by Chang and Brate [34]. Since the main goal is achieved large crystals, the optimization should avoid seeding in order to get a crystal with large size. Therefore, Moulin [35] provided a temperature control route to fix the seeding in a low level. Because of the non-linear dependency of seeding and the growth rate of super-saturation, it is essential to continue the growth and seeding by keeping the super-saturation in a low level. This is a suitable and desired trend which is followed by Jones and Moulin [36]. Ray and Ajinkya [37] used the functional optimization of the sulfate ammonium model to maximize the mean crystal size and obtain the optimal temperature profile. Moreover, Moulin [36] investigated the role of temperature control on the liquid solution of potassium and sulfate ammonium to maximize the final size of the crystals. In addition, the researchers found that the speed of the primary cooling is too slow in this curve while the cooling rate is much greater at the end of the cooling [38].

Jones and Moulin [36] used the optimal control theory to find an optimized cooling profile by using the momentum way for independent population balance. This research confirmed that the optimized cooling profile is achieved when the mean crystal size increases in contrast to cooling linear strategies. Hu et al. [39] worked to find a temperature profile in order to obtain the objective functions of the product in the final time. By using population balance idea, a new method is presented to solve the population balance in the crystallization process. Moreover, optimized algorithm finds the quantified value of the objective function for an input temperature parameter. Finally, they presented the results for the natural cooling, linear cooling and optimal cooling.

In this work, the batch cooling crystallization procedure is investigated to develop an appropriate optimization strategy. The influence of solubility is studied to characterize the temperature of batch cooling crystallization. In order to produce a product with high purity, parameter size distribution and suitable shape crystal, the temperature profile should be optimized for the crystallization process. Temperature control policy is necessary in the batch cooling crystallization to provide a suitable crystal size distribution for the product through the optimization. Hence, batch cooling crystallization is initially modeled. Then, objective functions are used to optimize the temperature of crystallization by the genetic algorithm. Maximum mean size, closeness to the desired value (desired mean weight size) and the minimum coefficient of variation

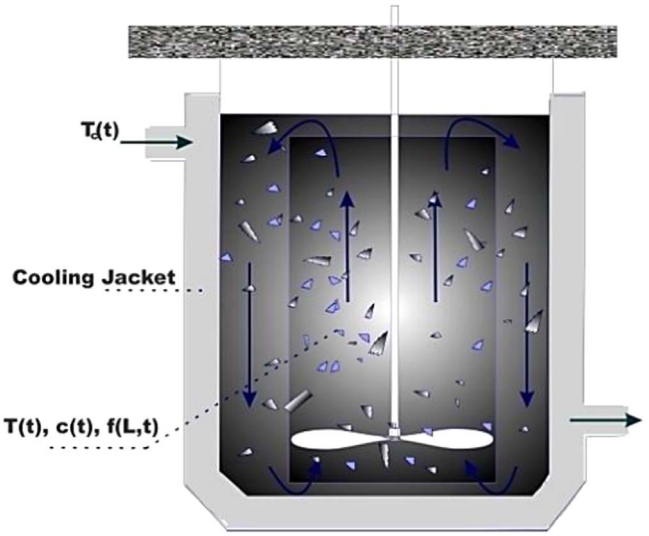

Fig. 1. Schematic Batch cooling crystallizer.

are used to optimize the temperature profile by this method. In fact, a genetic algorithm with new objective functions is employed to obtain optimum trends of the temperature variation in the batch crystallizer.

2. Population balance for batch crystallizer

As the crystallization process is a particulate one, various researchers [40,41] proposed the population balance theory as an approach for modeling of the crystallization process. This theory proposes the use of a balance to account for the number of crystals in the crystallizer. The output of such a balance is a distribution of the number of crystals across both time and size domains.

The scheme of batch cooling crystallizer is shown in Fig. 1. Initially, the vessel is filled with hot under-saturated solution. Next, the crystallizer is cooled when the liquid becomes supersaturated. At this point, small seed crystals are added. Due to the super - saturation condition, new crystals are formed and existing crystals simultaneously grow. The nucleation and growth consume solute from the solution. Hence, the concentration of the solution decreases. Therefore, further cooling is necessary to keep the liquid supersaturated. To prevent the settling of crystals, the slurry is mixed by an impeller. Finally, the vessel is discharged and the crystalline product undergoes further processing steps such as filtering and drying. The quality of the product as well as the efficiency of downstream processing is highly influenced by the CSD.

It is assumed that the rate of growth (G) is not related to the size of the crystal. The attrition, breakage and the agglomeration of crystal are negligible in this model. The equation of the population balance with boundary and initial conditions for the batch crystallization is presented as the follows [17]:

$$\frac{\partial f(L,t)}{\partial t} = -\frac{\partial\left(G(t)f(L,t)\right)}{\partial L} \tag{1-a}$$

$$f(0,t) = \frac{B(t)}{G(t)} \tag{1-b}$$

$$f(L,0) = f_{seed}(L) \tag{1-c}$$

The rate of nucleation is denoted by B(t), and f_{seed} (l) is the crystal size distribution of seed crystals.

By defining a mole equation of the liquid phase, an integro-differential equation will be obtained for the solute concentration:

$$\frac{dc(t)}{dt} = -3\rho_c k_v \int_0^\infty L^2 G(t) f(L,t)\,dL \tag{2}$$

This equation(Eq. (2)) is solved with the initial condition $C(0)=C_0$. In equation, ρ_c is the crystal density, k_v is the bulk density coefficient. A volume of crystal is defined as follows:

$$V_{crystal} = kvL^3 \tag{3}$$

Wherein, L is the size of the crystals.

Furthermore, the energy balance of the crystallizer determines an ODE of temperature T(t) as follows:

$$\rho V C_p(t)\frac{dT(t)}{dt} = -3\Delta H_c(t)\rho_c k_v \int_0^{\infty} L^2 G(t) f(L,t)dL - UA_c\left(T(t) - T_c(t)\right) \tag{4}$$

With T(0)= T_0. T_c(t) is the temperature of the cooling jacket, U represents the heat-transfer coefficient, A_c is heat transfer area, and ρ is the density of the slurry. The heat of crystallization, ΔH_c, depends on solution concentration c(t). This relation can be adequately represented by a quadratic term,

$$\Delta H_c(t) = B_0 + Bc(t) + B_2 c(t)^2 \tag{5}$$

Where the coefficients B_i, i=0, …, 2, are fitted to empirical data. Similarly, the heat capacity of the solution as a function of solution concentration can be expressed as:

$$C_p = C_0 - C_1\left(\frac{\hat{C}}{1+\hat{C}}\right) + C_2\left(\frac{\hat{C}}{1+\hat{C}}\right)^2 \tag{6}$$

The rate of growth and nucleation with super-saturation S(t), and f(L,t) are as follows:

$$G(t) = k_g S(t)^g \tag{7}$$

$$B(t) = k_b S(t)^b k_v \int_0^{\infty} L^3 G(t) f(L,t)dL \tag{8}$$

Where:

$$S(t) = \frac{C(t) - C_{sat}(t)}{C_{sat}(t)} \tag{9}$$

The relation of the saturation density C_{sat} (t) and temperature is estimated with a second order equation as follow:

$$C_{sat}(t) = A_0 + A_1 T(t) + A_2 T(t)^2 \tag{10}$$

The growth and nucleation laws (Eqs. 7 and 8) are empirical relations, and they are not derived directly from first principles. The value of b, g, k_b and k_g parameters are obtained through an identified system. The Eqs. (1-a) to (4) present a model with limited dimensions to analyze the batch crystallizer that mainly consists of a first order partial differential equation. Randolph and Larson [17] presented a new method for reducing the population balance equation to a set of ordinary differential equations. This method changes the partial differential equation to some ordinary ones as follow:

$$\mu_i(t) = \int_0^{\infty} L^i f(L,t)dL \quad i=0, 1, 2, \ldots \tag{11}$$

Eq. (7) is known as a momentum derived through physical interpretations. In fact, the zeroth order of the moment μ_0(t) defines the overall number of the crystals. In addition, the 1st (μ_1(t)), 2nd (μ_2(t)) and 3rth (μ_3(t)) order of the moment present the length of the crystal, the overall crystal surface and the volume of the crystalline inside the crystallizer, respectively. Since the final time of batch and the rate of growth are so limited, f(L,t) is zero for a high length. Therefore, following equations are obtained through an integration of the Eqs. (1-a) and (1-b):

$$\frac{d\mu_0(t)}{dt} = B(t) \tag{12-a}$$

$$\frac{d\mu_i(t)}{dt} = iG\left(\mu_3(t), T(t)\right)\mu_{i-1}(t) \quad i=1, 2, \ldots \tag{12-b}$$

Since the overall mass of solute (dissolved and crystalline) is constant in the crystallizer, an additional algebraic relation between the third moment μ_3(t) and the solute concentration c(t) is presented as follows [4,7]:

$$c(t) = c_0 + \rho_c k_v h(\mu_{3,seed} - \mu_3(t)) \tag{13}$$

Where $\mu_{3,seed} = \int_0^{\infty} L^i f_{seed}(L)dL$ is the third moment of the seed crystal size distribution. The nucleation law (Eq. (7)) is obtained as follow:

$$B(t) = k_b k_v S(t)^b \mu_3(t) \tag{14}$$

Eq. (10) shows that B(t) and G(t) are related to μ_3(t) and T(t). Then, the differential equations for the first six moments are as follow:

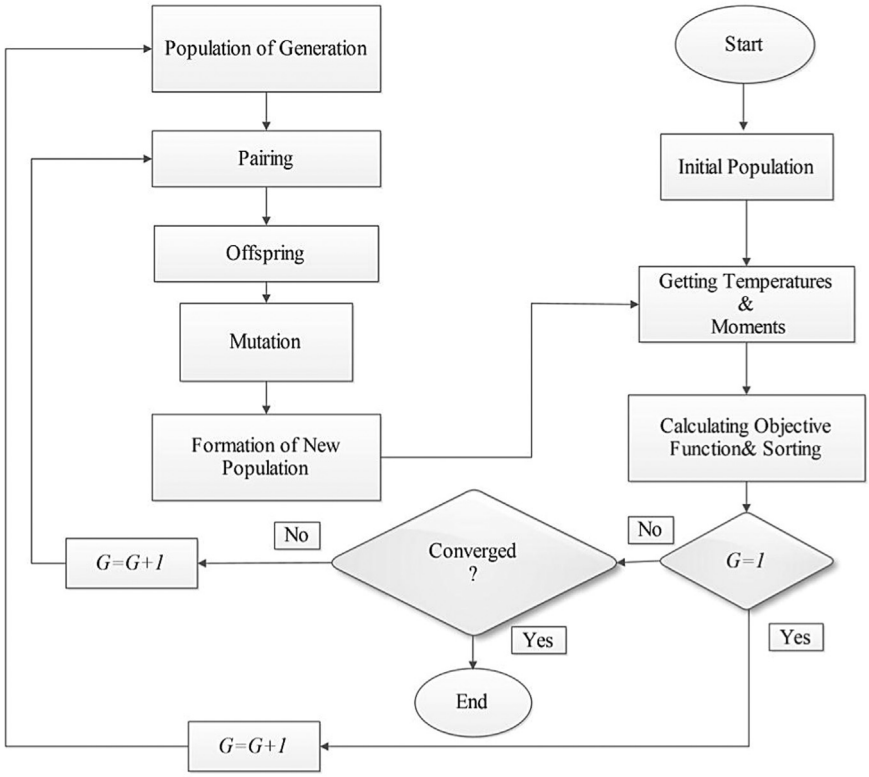

Fig. 2. Flowchart of Genetic Algorithm.

$$\frac{d\mu_0(t)}{dt} = B\left(\mu_3(t), T(t)\right) \tag{15-a}$$

$$\frac{d\mu_1(t)}{dt} = G\left(\mu_3(t), T(t)\right)\mu_0(t) \tag{15-b}$$

$$\frac{d\mu_2(t)}{dt} = 2G\left(\mu_3(t), T(t)\right)\mu_1(t) \tag{15-c}$$

$$\frac{d\mu_3(t)}{dt} = 3G\left(\mu_3(t), T(t)\right)\mu_2(t) \tag{15-d}$$

$$\frac{d\mu_4(t)}{dt} = 4G\left(\mu_3(t), T(t)\right)\mu_3(t) \tag{15-e}$$

$$\frac{d\mu_5(t)}{dt} = 5G\left(\mu_3(t), T(t)\right)\mu_4(t) \tag{15-f}$$

$$\frac{dT(t)}{dt} = -\frac{3\rho_c k_v}{\rho}\frac{\Delta H_c\left(\mu_3(t)\right)G\left(\mu_3(t), T(t)\right)\mu_2(t)}{c_p\left(\mu_3(t)\right)} - \frac{UA_c}{\rho V}\frac{(T - T_c)}{c_p\left(\mu_3(t)\right)} \tag{15-g}$$

With the initial conditions:

$$\mu_i(0) = \mu_{i,seed} = \int_0^\infty L^i f_{seed}(L)dL \quad i=0, \ldots, 5 \tag{15-h}$$

These equations are a simple model for the batch crystallizer, and it is clear that they are non-linear equations. The $\mu_0(t)$, …, $\mu_5(t)$ moments are the simplified model of our problem.

The number of density function was defined by f(L) and, mean weight size L_{wm} expressed as the following:

$$L_{wm} = \frac{\int_0^\infty L^4 f(L)dL}{\int_0^\infty L^3 f(L)dL} = \frac{\mu_4}{\mu_3} \tag{16}$$

In discrete condition, Eq. (12) transform to following equation.

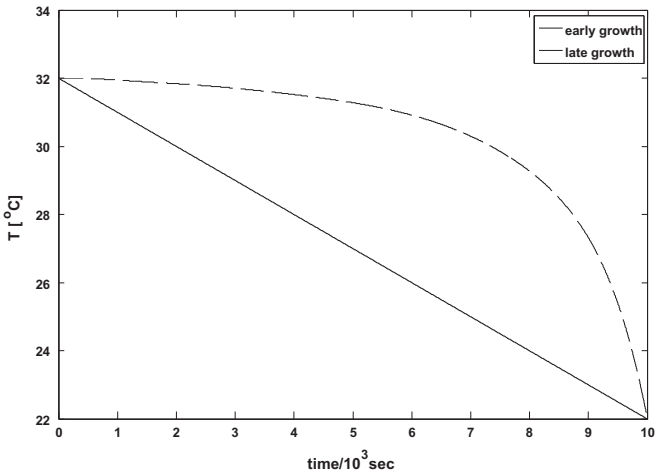

Fig. 3. Early-growth and late-growth temperature trajectories.

$$L_{wm} = \frac{\sum_{i=1}^{n} L_i w_i}{\sum_{i=1}^{n} w_i} \tag{17}$$

where w_i is crystal weight on *i*th mesh and L_i is the mean size of that mesh. The coefficient of variation (C.V) is expressed as the follow:

$$C.V = \frac{\sigma}{L_{wm}} \tag{18}$$

where σ (standard deviation) or σ^2 (variance) are obtained based on the moments model as the following:

$$\sigma^2 = \frac{\mu_5\mu_3 - \mu_4^2}{\mu_3^2} \tag{19}$$

$$\sigma = \frac{1}{\mu_3}\sqrt{\mu_5\mu_3 - \mu_4^2} \tag{20}$$

The coefficient of variation is expressed as the following dimensionless number.

$$C.V = \frac{\sigma}{L_{wm}} = \sigma\frac{\mu_3}{\mu_4} = \sqrt{\frac{\mu_5\mu_3}{\mu_4^2} - 1} \tag{21}$$

3. Optimization by using genetic algorithm

Genetic algorithms present the compatible framework to deal with the wide range of optimization problems [42–44]. Inspired from the evolutionary theory of Darwin, the algorithm introduces a population of possible solutions like the natural evolution of generations. Wherein, problem variables are represented as real strings, and the solution is coded as a collection (similar to chromosome) of these binary strings. The evolution is obtained by some genetic operators as a reproduction, crossover and mutation.

Recently, genetic algorithm is highly considered as the main method for optimization based on the mathematical modeling of the development theory. A genetic algorithm is applied to determine the optimal operating conditions for the crystallization process. Genetic algorithms are mathematical optimization methods that simulate a natural evolution process. The goal of this work is to optimize the temperature of crystallization process. The temperature is an important parameter and changes during the time for the process, an optimized temperature exists for further production. It has a direct effect on concentration.

In the genetic algorithm, the chromosome includes a set of data for the parameters and optimization variables, which is used to optimize the mathematical equations (quantitative equations). If the problem has N_{par} parameters and P is the parameter, the chromos used in the algorithm is as the following:

$$chromosome=[P_1, P_2,\ldots,P_{N_{par}}] \tag{22}$$

where $_{Pi}$ and N_{par} include the genes related to the chromosomes and the dimensions of the problem, respectively. In this

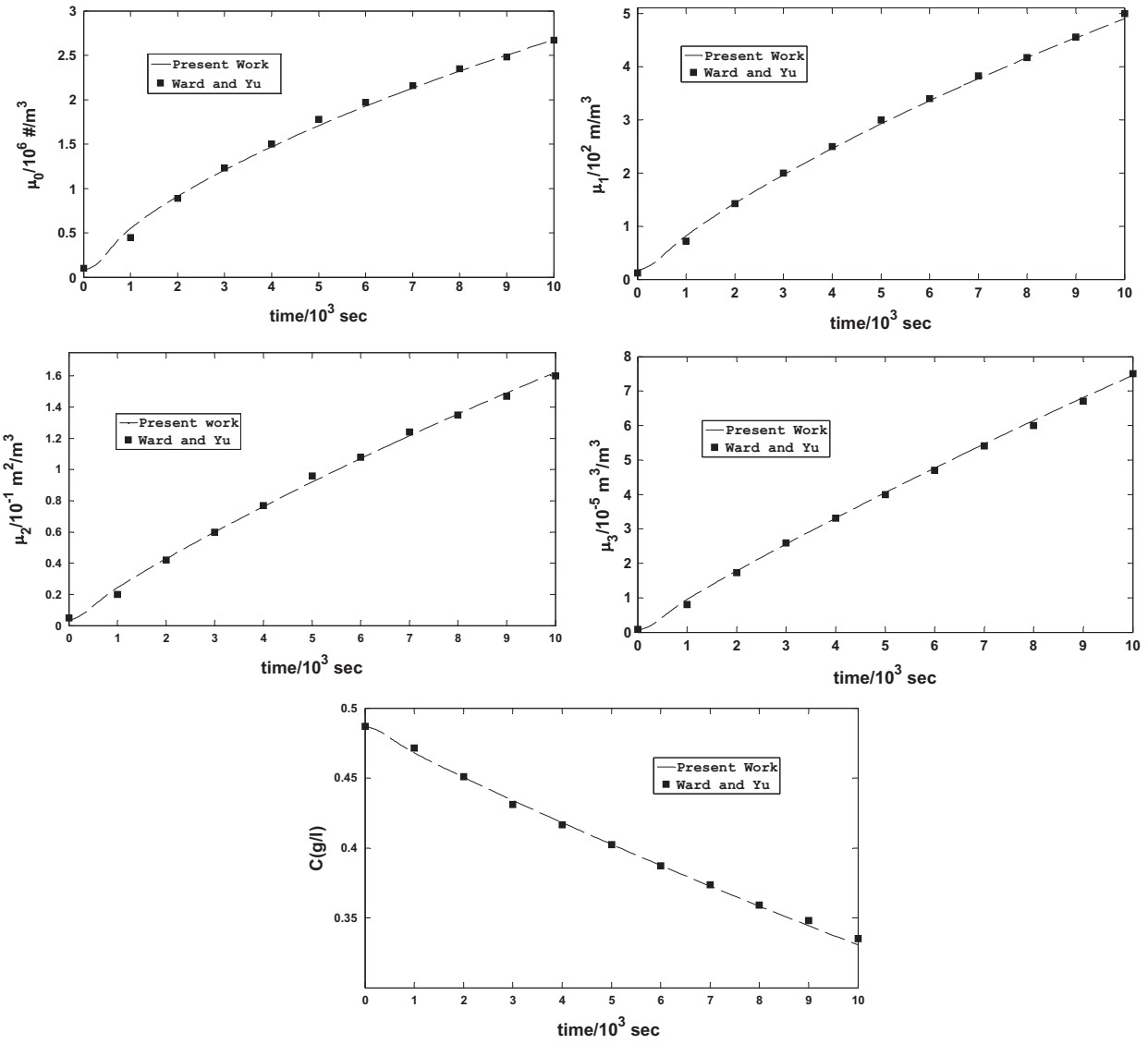

Fig. 4. Validation of time evolution of the solute concentration and the first four moments of the crystal size distribution function for early-growth operating policies as calculated by using the method of moments and Ward and Yu [28].

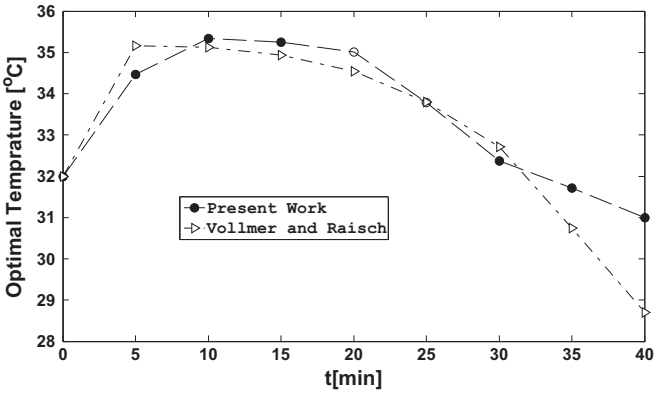

Fig. 5. Optimal temperature versus time for maximum mean weight size.

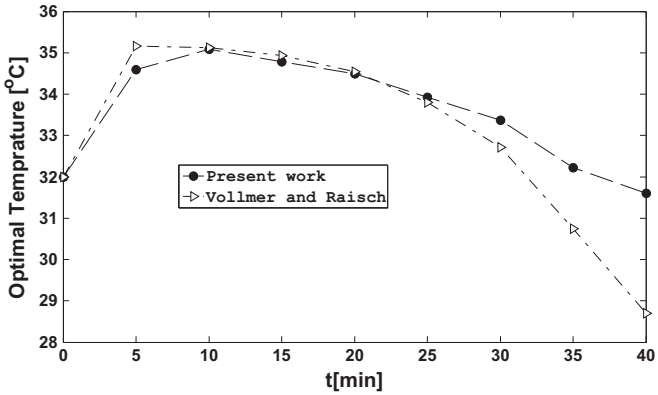

Fig. 6. Optimal temperature versus time for closeness to the specified value.

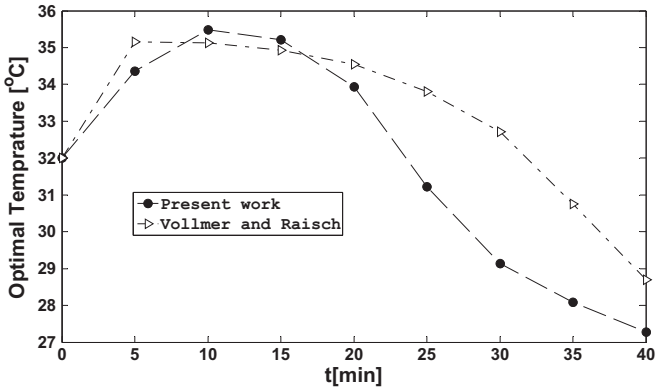

Fig. 7. Optimal temperature versus time for minimum coefficient of variation.

Table 1
Relative error between optimal temperature with feedforward control and optimal temperature with genetic algorithm data.

Objective function	**MARE (%)** $=100\frac{1}{N}\sum\left\|1-\frac{Y_{OPT}}{Y_V}\right\|$
maximum mean weight size	**2.46**
closeness to the specified value	**2.37**
minimum coefficient of variation	**4.85**

optimization method, a lot of chromosomes are produced and, the optimum chromosomes will be attained by a re-population and mutation.

4. Objective functions

There is a great deal of subtlety associated with selecting an objective function for seeded batch crystallizers. Part of the problem, as several researchers have noted, is that it may be difficult to correlate the cost of downstream processing to the crystal-size distribution. As a result, it has not generally been practical to use process economics to formulate an objective. Consequently, researchers have been forced to identify a surrogate objective function based on some property of the crystal-size distribution.

Researchers [19,24–28] have presented many different objective functions for the cooling crystallization. In this study, three objective functions are used for the optimization of the batch cooling crystallization. These functions (objective function of maximum mean weight size, closeness to the specified value and minimum coefficient of variation) are discussed as follow:

4.1. Objective function of maximum mean weight size

This function is based on the mean size of the crystals and at the end of the batch the largest crystals make the largest mean size that is:

$$ObjectiveFunction1{=}MaxL_{wm}\left(t_f\right) = Max\int_o^{t_f} G\left(4 - 3\frac{\mu_4\mu_2}{\mu_3^2}\right)dt \tag{23}$$

4.2. Objective function of closeness to the specified value (desired mean weight size)

This function is based on the amount of closeness to the predetermined mean length such that at the end of the batch, the mean weight size is closer to the specified value that is:

$$ObjectiveFunction2{\equiv}\int_0^{t_f} 2G\frac{\mu_4}{\mu_3}\left|L_{wm}\left(t_f\right) - L_{wm}^{d}\right|\left(4 - 3\frac{\mu_4\mu_2}{\mu_3^2}\right)dt \tag{24}$$

4.3. Objective function of minimum coefficient of variation

This objective function is based on the minimum coefficient of variation such that the lowest coefficient of variation is seen at the end of the batch. In other words, we want to have a very sharp and narrow curve of the crystals sizes distribution that is:

$$ObjectiveFunction3 \equiv \mathrm{Min}C.\ V\left(t_f\right){=}\mathrm{Min}\int_0^{t_f} \frac{G\mu_3}{2\sqrt{\frac{\mu_3\mu_5}{\mu_4}-1}}\left(\left(\frac{3\mu_5\mu_2}{\mu_3} + 5\mu_4\right) - \frac{8\mu_5\mu_3}{\mu_4}\right)dt \tag{25}$$

5. Applying genetic algorithm to obtain the optimal temperature

As the genetic algorithm applied in the robust objective function subjected to operating constraints for the full range of uncertain parameters, the optimal temperature trajectory is determined. In the present problem of optimization, the relevant chromosome is initially determined. Since the genetic algorithm is a time consuming process, the end of the batch is classified into eight time periods of five-minute sets. The chromosome is identified as the combination of eight continuous genes (D_i) which are randomly assessed by discrete value between zero to one as the followings:

$$chromosome{=}[D_1, D_2, D_3, D_4, D_5, D_6, D_7, D_8] \tag{26}$$

Since the obtained genes are normalized, the measurement of the objective function is performed by using the maximum and minimum values of the calculated parameters. To select appropriate pairs, the random weighted selection method is applied. This method is based on the cost function of the chromosomes. Next, the extrapolation method with two cutting points is used for the recombination of the chromosomes. In this methodology, two random chromosomes are selected from the parents and then combined together with a random weight. The typical flowchart of the employed genetic algorithm in the solution of the models is given in the Fig. 2.

Initial temperature and concentration parameters are considered as 32 °C and 0. $5733\frac{gKNO_3}{gH_2O}$, respectively. Ode23s tool in the MATLAB computation software is used to solve the equations. For this purpose, the initial population and mutation coefficient are adjusted between 40–1000, and 0.02–20, respectively. Finally, the optimal temperature profile is calculated for each objective function by using the identified algorithm.

6. Results and discussion

Ward et al. [28] introduce the concepts of “early growth” and “late growth” for the selection of operating policies for seeded batch crystallization where secondary nucleation is important (Eq. (14)). In an early-growth operating policy, the growth rate (supersaturation) is the greatest at the beginning of the batch. However, it is greatest at the end of the batch when a late growth operating policy is done [28,29]. For cooling crystallization, the rate of change of temperature is the greatest in an absolute sense at the beginning of a batch for early growth and at the end of the batch for late growth. Ward et al. predicted that early-growth operating policies should produce a smaller *number* of the nucleus grown crystals, but a greater *mass* of the nucleus-grown crystals. A late-growth operating policy should produce a greater number but a smaller mass of the nucleus-grown crystals and at the same time grow the seed crystals to a larger size. The reader is referred to Ward et al. [28] for a detailed explanation of why this should be the case. This paper will develop further insight into this

result by providing the complete population density function at the end of a batch for a seeded batch crystallizer subjected to early-growth and late-growth operating policies.

Fig. 3 shows the temperature trajectories used in this problem. Note that the early-growth trajectory has a high slope in an absolute sense at the commence of the batch while the late-growth trajectory has a slope steepest in an absolute sense at the end of the batch. Although the early-growth trajectory is nearly linear, it results in a significantly greater super saturation at the beginning of the batch than at the end of the batch.

Fig. 4 clearly shows the time evolution of the first four moments of the population density function for the early-growth operating policies as calculated and the method of moments. Moreover, in this figure time evolution of the solute concentration and the first four moments of the crystal size distribution function for early-growth operating have been validated with Ward and Yu [28]. The lines overlap almost exactly, suggesting that the simulation gives a very accurate description of the time evolution of the population density function. It is also noted that the moments grow rapidly at the beginning of the batch because of used of the early-growth operating policy.

The same optimum solution as that given by Vollmer and Raisch [29] was obtained with feed forward control. In this study, after about 200 generation the size of initial population was 1000 chromosomes and the maximum number of generations was set to 1000.

Following constraints are given to the objective functions in the genetic algorithm:

$$T_{min} \le T \le T_{max},\ C_{sat} \le C \le C_{max}$$

Where minimum and maximum temperatures are 27 °C and 37 °C, respectively.

The objective functions are maximum mean weight size, closeness to the specified value and minimum coefficient of variation.

The obtained optimal temperature profile from the maximum mean weight size objective function is shown in the Fig. 5. In this figure optimal temperature have been validated with vollmer and Risch [41]. The figure evaluates the optimal temperature against time. It can be easily observed that both genetic algorithm and feed forward control results present similar temperature trends when the time passed. It is notable that the temperature rises sharply and this is because of difference between initial concentration and the supersaturated concentration. As the time passes, the difference decreases.

The obtained optimal temperature profile from the closeness to the specified value objective function and validation with the vollmer and Risch [41] are shown in Fig. 6. It can be easily observed that both genetic algorithm and feedforward control results present similar temperature trends when the time passed. In the beginning of the batch process the temperatures closes to optimal control. It is notable that the differences between temperatures at the end of the process are raised in compare to maximum mean weight size objective function.

The obtained optimal temperature profile from the minimum coefficient of the variation objective function and validation with the vollmer and Risch [41] are shown in Fig. 7. It can be easily observed that both genetic algorithm and feed forward control results present similar temperature trends as the time passed. In this objective function, the differences between the temperatures are raised.

The relative error between optimal temperature with feedforward control and optimal temperature with genetic algorithm data are shown in Table 1. As it can be seen, minimum error is occurred in the vicinity of the specified value objective function. Since, this objective function presented at the first time, results of this function are close to the optimal value.

As eight parameters should be optimized in this case, the initial population is increased from 40 to 1000 to ensure the search in all domains. The optimal number of the initial population is 200. For lower values, it does not search the entire domain of optimization that is due to the low number of the population. As the initial population is increased, extra recombination in chromosomes causes an increase in the cost. In order to get the best mutation coefficient for the initial population of 200 (best initial population), mutation is varied from 0.02 to 0.2. The optimal value for mutation coefficient in this condition is 0.05.

7. Conclusion

In this work, the batch cooling crystallization procedure is investigated to develop an appropriate optimization strategy. The influence of the solubility is studied to characterize the temperature of batch cooling crystallization. Temperature control policy is necessary in the batch cooling crystallization to provide a suitable crystal size distribution for the product through the optimization. Hence, batch cooling crystallization is initially modeled. Then, objective functions are used to optimize the temperature of crystallization through a genetic algorithm. Maximum mean size, closeness to the desired value (desired mean weight size) and the minimum coefficient of variation are applied to optimize the temperature profile by the genetic algorithm. Results show that the desired value objective function that is presented in the first time is the best objective function. The mean relative error of this objective function is lower than other functions that presented in this study.

References

[1] A. Mesbah, A.E.M. Huesman, H.J.M. Kramer, P.M.J. Van den Hof, A comparison of nonlinear observers for output feedback model-based control of seeded batch crystallization processes, J. Process Control 21 (2011) 652–666.
[2] A.G. Jones, J.W. Mullin, Programmed cooling crystallization of potassium sulphate solutions, Chem. Eng. Sci. 29 (1974) 105.
[3] Sh Qamar, S. Mukhtar, A. Seidel-Morgenstern, M. Peter Elsner, An efficient numerical technique for solving one-dimensional batch crystallization models with size-dependent growth rates, Chem. Eng. Sci. 64 (2009) 3659–3667.
[4] S.M. Nowee, A. Abbas, J.A. Romagnoli, Antisolvent crystallization: Model identification, experimental validation and dynamic simulation, Chem. Eng. Sci. 63 (2008) 5457–5467.
[5] O. Velazquez-Camilo, E. Bolanos-Reynoso, E. Rodriguez, J. Alvarez-Ramirez, Fractal analysis of crystallization slurry images, J. Cryst. Growth 312 (2010) 842–850.
[6] A. Saengchan, P. Kittisupakorn, W. Paengjuntuek, A. Arpornwichanop, Improvement of batch crystallization control under uncertain kinetic parameters by model predictive control, J. Ind. Eng. Chem. 17 (2011) 430–438.
[7] S.M. Miller, J.B. Rawlings, Model identification and control strategies for batch cooling crystallizers, AIChE J. 40 (1994) 1312–1327.
[8] H.B. Matthews, J.B. Rawlings, Batch crystallization of a photochemical modeling, control and 7ltration, AIChE J. 44 (1998) 1119–1127.
[9] N. Doki, M. Yokota, K. Kido, S. Sasaki, N. Kubota, Reliable and selective crystallization of the metastable-form glycine by seeding, Cryst. Growth Des. 4 (2004) 103–107.
[10] W.L. McCabe, J.C. Smith, P. Harriot, Unit Operations of Chemical Engineering, McGraw Hill Inc, New York, 1998.
[11] M. Ajinkya, W. Ray, On the optimal operation of crystallization processes, Chem. Eng. Comm. 1 (1974) 181–186.
[12] A. Jones, Optimal operation of a batch cooling crystallizer, Chem. Eng. Sci. 29 (1974) 1075–1087.
[13] M. Ulrich, Optimization of batch solution crystallization, Ger. Chem. Eng. 4 (1979) 195–200.
[14] B. Mayrhofer, J. Nyvlt, Programmed cooling of batch crystallizers, Chem. Eng. Process. 24 (1988) 217–220.
[15] Y. Lang, A. Cervantes, L. Biegler, Dynamic optimization of a batch cooling crystallization process, Ind. Eng. Chem. Res. 38 (1999) 1469–1477.
[16] M.B. Gerdroodbary, M. Rahimi, D.D. Ganji, Investigation of thermal radiation on traditional Jeffery-Hamel flow to stretchable convergent/divergent channels, Case Stud. Thermal Eng. 6 (2015) 28–39.
[17] M.B. Gerdroodbary, M. Imani, D.D. Ganji, Investigation of film cooling on nose cone by a forward facing array of micro-jets in Hypersonic flow, Int. Commun. Heat. Mass Transf. 64 (2015) 42–49.
[18] M.B. Gerdroodbary, D.D. Ganji, Y. Amini, Numerical study of shock wave interaction on transverse jets through multiport injector arrays in supersonic crossflow, Acta Astronaut. 115 (2015) 422–433.
[19] M. Barzegar Gerdroodbary, O. Jahanian, M. Mokhtari, Influence of the angle of incident shock wave on mixing of transverse hydrogen micro-jets in supersonic crossflow, Int. J. Hydrog. Energy 40 (2015) 9590–9601.
[20] Y. Amini, J. Karimi-Sabet, M. Nasr Esfahany, Experimental and numerical simulation of dry pressure drop in high-capacity structured packings, Chem. Eng. Technol. 39 (6) (2016) 1161.
[21] Y. Amini, J. Karimi-Sabet, M. Nasr Esfahany, Experimental and numerical study of multiphase flow in new wire gauze with high capacity structured packing, Chem. Eng. Proc.: Proc. Intensif. 108 (2016) 35–43.
[22] R. Moradi, J. Karimi-Sabet, M. Shariaty-Niassar, Y. Amini, Air gap membrane distillation for enrichment of H 2 18O isotopomers in natural water using poly (vinylidene fluoride) nanofibrous membrane, Chem. Eng. Proc.: Proc. Intensif. 100 (2016) 26.
[23] Y. Amini, M. Haghshenasfard, M. Mokhtari, M.B. Gerdroodbary, Heat transfer of swirling impinging jets ejected from nozzles with twisted tapes utilizing CFD technique, Case, Stud. Therm. ENG 6 (2015) 104.
[24] A. Sadeghi, Y. Amini, M.H. Saidi, H. Yavari, Shear-rate-dependent rheology effects on mass transport and surface reactions in biomicrofluidic devices, AIChE J. 61 (6) (2015) 1912–1924.
[25] A. Sadeghi, Y. Amini, M.H. Saidi, S. Chakraborty, Numerical modeling of surface reaction kinetics in electrokinetically actuated microfluidic devices, Anal. Chim. Acta 838 (2014) 64–75.
[26] S.V. Mousavi, M. Sheikholeslami, M. Gorji bandpey, M.B. Gerdroodbary, The influence of magnetic field on heat transfer of magnetic nanofluid in a sinusoidal double pipe heat exchanger, Chem. Eng. Res. Des. 113 (2016) 112–124.
[27] M.B. Gerdroodbary, M.R. Takami, H.R. Heidari, K. Fallah, D.D. Ganji, Comparison of the single/multi Transverse jets under the influence of shock wave in Supersonic Crossflow, Acta Astronaut. 123 (2016) 283–291.
[28] R. Gunawan, D.L. Ma, M. Pujiwara, R.D. Braatz, Identification of kinetic parameters in a multidimensional crystallization process, Int. Y. Mod. Phys. B 16 (2002) 367–374.
[29] D.L. Ma, R.D. Braatz, Robust batch control of crystallization processes, in: Proceedings of the American Control Conference, IEEE Press, Piscataway, New Jersey, 2000, pp. 1737–1741.
[30] T.P. Redman, S. Rohani, G. Strathdee, On-line control of supersaturation in a continuous cooling KCl crystallizer, Can. J. Chem. Eng. 73 (1995) 725–733.
[31] C.T. Chang, M. Epstein, Simulation studies of a feedback control strategy for batch crystallizers, AICh ESymp. Ser. 83 (1987) 110–119.
[32] S. Motz, J. Eggers, E. Gilles, Model-based operation of batch crystallizers, in: Proceedings of the 15th International Symposium on Ind. Cryst., 3, 2002, pp. 1173–1179.
[33] G. Zhang, S. Rohani, On-line optimal control of a seeded batch crystallizer, Chem. Eng. Sci. 58 (2003) 1887–1896.
[34] S. Chung, D. Ma, R. Braatz, Optimal seeding in batch crystallization, Can. J. Chem. Eng. 77 (1999) 590–596.
[35] J. Mullin, J. Nyvlt, Programmed cooling of batch crystallizers, Chem. Eng. Sci. 26 (1971).
[36] A. Jones, J. Mullin, Programmed cooling crystallization of potassium sulphate solutions, Chem. Eng. Sci. 29 (1974) 105–118.
[37] M.B. Ajinkya, W.H. Ray, On the optimal operation of crystallization processes, Chem. Eng. Commun. 1 (1974) 181.
[38] A. Jones, J. Mullin, Programmed cooling crystallization of potassium sulphate solutions, Chem. Eng. Sci. 29 (1974) 105–118.
[39] Q. Hu, S. Rohani, D.X. Wang, A. Jutan, Optimal control of a batch cooling seeded crystallizer, Powder Technol. 156 (2005) 170–176.
[40] J.D. Ward, C. Yu, Population balance modeling in Simulink: PCSS, Comput. Chem. Eng. 32 (2008) 2233–2242.
[41] U. Vollmer, J. Raisch, Control of batch crystallization-a system inversion approach, Chem. Eng. Process. 45 (2006) 874–885.
[42] K. Deb, A. Pratap, S. Agarwal, T. Meyarivan, A fast and elitist multi objective genetic algorithm: NSGA-II, IEEE Trans. Evolut. Comput. 6 (2002) 182–197.
[43] Y. Amini, M. Fattahi, F. Khorasheh, S. Sahebdelfar, Neural network modeling the effect of oxygenate additives on the performance of Pt–Sn/γ-Al2O3 catalyst in propane dehydrogenation, Appl. Petrochem. Res. 3 (2013) 47–54.
[44] C.M. Silva Jr., E.C. Biscaia, Genetic algorithm development formulation objective optimization of batch free-radical polymerization reactors, Comput. Chem. Eng. 27 (2003) 1329–1344.